

An Optimization-Based Perturbed Newton Method for Viscoplastic Fluids with von Mises Yielding

Johann Rudi¹ Georg Stadler² Omar Ghattas³

¹Mathematics and Computer Science Division, Argonne National Laboratory

²Courant Institute of Mathematical Sciences, New York University

³Oden Institute, Jackson School of Geosciences, and Dept. of Mechanical Engineering,
The University of Texas at Austin



Outline

Introduction

Derivation of Locally Perturbed Newton Linearizations

Earth's Mantle Convection: Driving Application & Solver Challenges

Numerical Experiments: Viscoplastic/Multi-Viscosity Stokes Flow

Implications and Outlook for Computational Mantle Flow

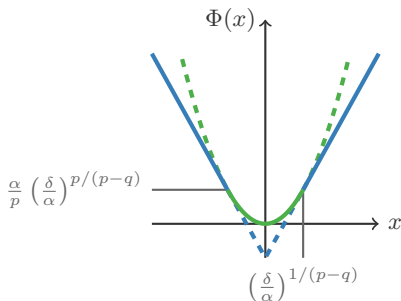
Introduction: Minimization problem

Find the minimizer $x^* \in \mathbb{R}$ of the problem

$$\min_x \Phi(x) := \begin{cases} \frac{\alpha}{p} |x|^p, & \alpha |x|^{p-q} \leq \delta, \\ \frac{\delta}{q} |x|^q + \gamma, & \text{otherwise,} \end{cases}$$

with given

- ▶ exponents $1 \leq q < p < \infty$
- ▶ parameters $\alpha, \delta > 0$
- ▶ $\gamma := \alpha \left(\frac{\delta}{\alpha}\right)^{p/(p-q)} \left(\frac{1}{p} - \frac{1}{q}\right)$

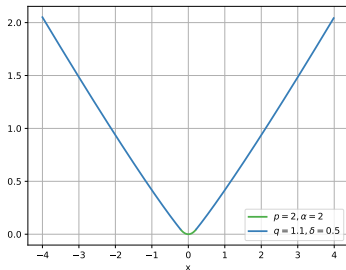


Introduction: Objective, gradient, and Hessian

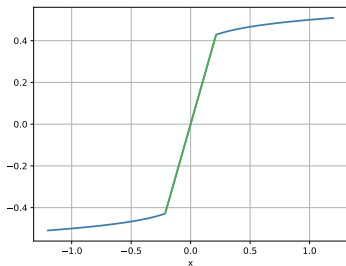
Parameters:

- ▶ $p = 2$
- ▶ $q = 1.1$
- ▶ $\alpha = 2$
- ▶ $\delta = 0.5$

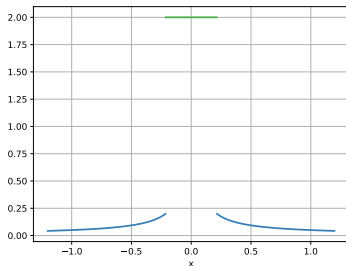
Objective Φ



Gradient Φ'

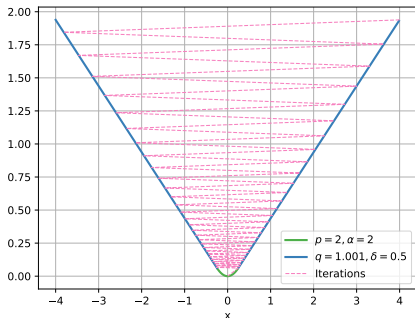


Hessian Φ''

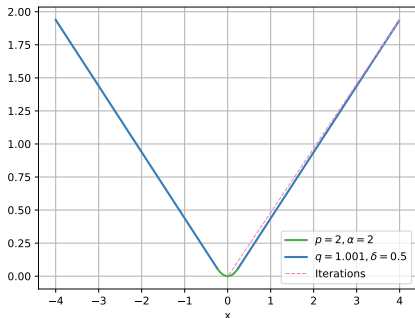


Introduction: Numerical experiments

Standard approach:
Newton: 59 iterations



Want:
Steepest Descend + Newton: 2 iterations



Parameters: $p = 2, q = 1.001, \alpha = 2, \delta = 0.5$

Outline

Introduction

Derivation of Locally Perturbed Newton Linearizations

Earth's Mantle Convection: Driving Application & Solver Challenges

Numerical Experiments: Viscoplastic/Multi-Viscosity Stokes Flow

Implications and Outlook for Computational Mantle Flow

Minimization problem

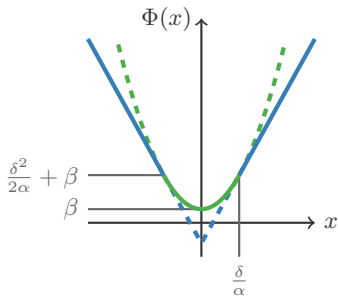
Given dimensions $d \in \mathbb{N}$ and $n \in \{1, d, d \times d\}$, domain $\Omega \subseteq \mathbb{R}^d$, and a linear and bounded functional $F : L^2(\Omega)^n \rightarrow \mathbb{R}$,

$$\text{find minimizer } U^* : \Omega \rightarrow \mathbb{R}^n \text{ of } \min_U J(U) := \int_{\Omega} \Phi(U) - F(U)$$

using a generalization of the *Huber loss*:

$$\Phi(U) := \beta + \begin{cases} \frac{\alpha}{2} |U|^2, & \alpha |U| \leq \delta, \\ \delta |U| - \frac{\delta^2}{2\alpha}, & \text{otherwise,} \end{cases}$$

with parameters $\alpha, \delta > 0$ and $\beta \in \mathbb{R}$.



Newton's method: A quadratic model of the nonlinearity

Goal: Construct a model of the nonlinear objective $J(U)$ locally around U . Newton's method approximates J with a Taylor expansion, truncated at the second-order term: (g and H are gradient and Hessian resp.)

$$J(U + \hat{U}) \approx J(U) + g(U)\hat{U} + \frac{1}{2} \left(H(U)\hat{U}, \hat{U} \right)$$

One Newton iteration involves:

1. **Solve** the linearized system for step \hat{U} (in variational form):

$$\left(H(U)\hat{U}, \tilde{U} \right) = -g(U)\tilde{U} \quad \text{for all } \tilde{U}$$

2. **Backtracking/line search** algorithm to find $\theta \in (0, 1]$ such that

$$J(U + \theta\hat{U}) < J(U) - \epsilon, \quad \text{for some fixed } \epsilon > 0$$

3. **Update** the solution: $U \leftarrow U + \theta\hat{U}$

Standard Newton linearization

The gradient and Hessian are the 1st- and 2nd-order variations of J :

$$g(U)\tilde{U} := \int_{\Omega} \left(\chi\alpha + (1 - \chi)\frac{\delta}{|U|} \right) \langle U, \tilde{U} \rangle - F(\tilde{U}), \quad \chi := \begin{cases} 1, & \alpha|U| \leq \delta, \\ 0, & \text{o.w.}, \end{cases}$$

$$(H(U)\hat{U}, \tilde{U}) := \int_{\Omega} \left\langle \left(\chi\alpha + (1 - \chi)\frac{\delta}{|U|} \left(\mathbf{I} - \frac{U \otimes U}{|U|^2} \right) \right) \hat{U}, \tilde{U} \right\rangle$$

The standard Newton linearization requires to solve for Newton step \hat{U} in

$$\int_{\Omega} \left\langle \left(\chi\alpha + (1 - \chi)\frac{\delta}{|U|} \left(\mathbf{I} - \frac{U \otimes U}{|U|^2} \right) \right) \hat{U}, \tilde{U} \right\rangle = -g(U)\tilde{U}$$

The outer product term is computationally challenging because:

- ▶ Coefficient $\left(\mathbf{I} - \frac{U \otimes U}{|U|^2} \right)$ in Hessian represents an **orthogonal projector**
- ▶ Hessian has a **zero eigenvalue** associated to eigenvector $(1 - \chi)U$

Locally perturbed Newton linearization

Introduce for $U, S \in L^2(\Omega)^n$

$$\text{Error term: } E(U, S) := \frac{U}{|U|} - S$$

$$\text{Perturbation: } D(U, S) := U - |U| S$$

We augment the previous gradient

$$g(U)\tilde{U} = \int_{\Omega} \left(\chi\alpha + (1 - \chi)\frac{\delta}{|U|} \right) \langle U, \tilde{U} \rangle - F(\tilde{U})$$

by a model perturbation, $D(U, S) \neq 0$,

$$g(U, S)\tilde{U} = \int_{\Omega} \langle \chi\alpha U + (1 - \chi)\delta S, \tilde{U} \rangle - F(\tilde{U})$$
$$(D(U, S), \tilde{S}) = \int_{\Omega} \langle U - |U| S, \tilde{S} \rangle$$

Locally perturbed and reduced Newton linearization

The **perturbed Newton linearization** for step (\hat{U}, \hat{S}) is

$$\int_{\Omega} \langle \chi \alpha \hat{U} + (1 - \chi) \delta \hat{S}, \tilde{U} \rangle = -g(U, S) \tilde{U}$$

$$\int_{\Omega} \left\langle \left(\mathbf{I} - \frac{U \otimes S}{|U|} \right) \hat{U} - |U| \hat{S}, \tilde{S} \right\rangle = - (D(U, S), \tilde{S})$$

and has an explicit expression for the dual step

$$\hat{S} = \frac{U}{|U|} - S + \frac{1}{|U|} \left(\mathbf{I} - \frac{U \otimes S}{|U|} \right) \hat{U}$$

Substitute to get the **perturbed and reduced Newton linearization** for \hat{U}

$$\int_{\Omega} \left\langle \left(\chi \alpha + (1 - \chi) \frac{\delta}{|U|} \left(\mathbf{I} - \frac{U \otimes S}{|U|} \right) \right) \hat{U}, \tilde{U} \right\rangle = -g(U) \tilde{U}$$

Improvements gained from perturbation

$$\int_{\Omega} \left\langle \left(\chi \alpha + (1 - \chi) \frac{\delta}{|U|} \left(\mathbf{I} - \frac{U \otimes U}{|U|^2} \right) \right) \hat{U}, \tilde{U} \right\rangle = -g(U) \tilde{U}$$

$$\int_{\Omega} \left\langle \left(\chi \alpha + (1 - \chi) \frac{\delta}{|U|} \left(\mathbf{I} - \frac{U \otimes S}{|U|} \right) \right) \hat{U}, \tilde{U} \right\rangle = -g(U) \tilde{U}$$

- ▶ Perturbation results in **model error dependent regularization**
- ▶ It maintains **fast Newton convergence** close to the solution

$$\mathbf{I} - \frac{U \otimes S}{|U|} = \mathbf{I} - \frac{U \otimes U}{|U|^2} + \frac{U \otimes E(U, S)}{|U|} \rightarrow \mathbf{I} - \frac{U \otimes U}{|U|^2} \quad \text{as } E(U, S) \rightarrow 0$$

- ▶ It acts as a **nonlinear preconditioner** far from the solution
- ▶ **Simple and computationally cheap** update of the dual variable S given \hat{U}

$$S \leftarrow S + \hat{S} = \frac{U}{|U|} + \frac{1}{|U|} \left(\mathbf{I} - \frac{U \otimes S}{|U|} \right) \hat{U}$$

Outline

Introduction

Derivation of Locally Perturbed Newton Linearizations

Earth's Mantle Convection: Driving Application & Solver Challenges

Numerical Experiments: Viscoplastic/Multi-Viscosity Stokes Flow

Implications and Outlook for Computational Mantle Flow

Earth's nonlinear rheology modeling the mantle & plates

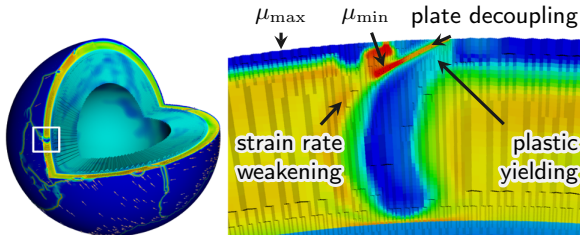
Nonlinear constitutive relationship / rheology due to:

- ▶ Strain rate weakening exponent $n \geq 1$ ($\dot{\epsilon}_{II}(\mathbf{u})$ is 2nd invariant of strain rate)
- ▶ Yield strength $\tau_{\text{yield}} > 0$ causing plastic yielding

Additional heterogeneity is introduced via:

- ▶ Exponential temperature dependence $a(T)$ (Arrhenius relationship)
- ▶ Plate decoupling factor $0 < w(\mathbf{x}) \leq 1$ with orders-of-magnitude contrasts

$$\mu_{\text{eff}}(T, \dot{\epsilon}_{II}(\mathbf{u})) := \mu_{\min} + \min \left(\frac{\tau_{\text{yield}}}{2\dot{\epsilon}_{II}(\mathbf{u})}, w(\mathbf{x}) \min \left(\mu_{\max}, a(T) \dot{\epsilon}_{II}(\mathbf{u})^{\frac{1}{n}-1} \right) \right)$$



Mantle flow governed by incompressible Stokes equations

Nonlinear incompressible Stokes PDE (w/ free-slip & no-normal flow BC):

$$\begin{aligned}
 -\nabla \cdot [2\mu(\dot{\epsilon}_{\text{II}}(\mathbf{u})) \dot{\epsilon}(\mathbf{u})] + \nabla p &= \mathbf{f} && \text{viscosity } \mu, \text{ RHS forcing } \mathbf{f} \\
 -\nabla \cdot \mathbf{u} &= 0 && \text{seek: velocity } \mathbf{u}, \text{ pressure } p
 \end{aligned}$$

Linearization (with Newton), then discretization (with inf-sup stable F.E.):

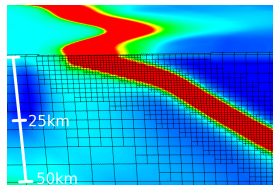
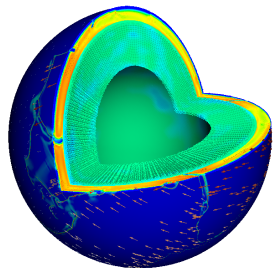
$$\begin{bmatrix} \mathbf{A} & \mathbf{B}^T \\ \mathbf{B} & \mathbf{0} \end{bmatrix} \begin{bmatrix} \hat{\mathbf{u}} \\ \hat{p} \end{bmatrix} = \begin{bmatrix} -\mathbf{r}_1 \\ -\mathbf{r}_2 \end{bmatrix}$$

- ▶ **High-order** finite element shape functions
- ▶ Inf-sup **stable velocity–pressure pairings**: $\mathbb{Q}_k \times \mathbb{P}_{k-1}^{\text{disc}}$ with order $k \geq 2$
- ▶ **Locally mass conservative** due to discontinuous, modal pressure
- ▶ **Non-conforming** hexahedral meshes with “hanging nodes”
- ▶ **Adaptive mesh refinement** resolving fine-scale features of mantle

Severe challenges for parallel scalable implicit solvers

... arising in global mantle convection:

- ▶ Severe **nonlinearity and heterogeneity** of Earth's rheology and **anisotropy** induced by it
- ▶ **Sharp viscosity gradients** in narrow regions (6 orders of magnitude drop in ~ 5 km)
- ▶ **Wide range of spatial scales** and **highly localized features**, e.g., plate boundaries of size $\mathcal{O}(1$ km) influence plate motion at continental scales of $\mathcal{O}(1000$ km)
- ▶ **Adaptive mesh refinement** is essential
- ▶ **High-order** finite elements $\mathbb{Q}_k \times \mathbb{P}_{k-1}^{\text{disc}}$, order $k \geq 2$, with **local mass conservation**; yields a difficult to deal with **discontinuous, modal pressure** approximation



Viscosity (colors) and locally refined mesh.

Outline

Introduction

Derivation of Locally Perturbed Newton Linearizations

Earth's Mantle Convection: Driving Application & Solver Challenges

Numerical Experiments: Viscoplastic/Multi-Viscosity Stokes Flow

Implications and Outlook for Computational Mantle Flow

Stokes flow with yielding rheology: Minimization problem

Given viscosity $\mu > 0$, yield strength $\tau_{\text{yield}} > 0$, the 2nd invariant of the strain rate tensor, $\dot{\epsilon}_{\text{II}} := \frac{1}{\sqrt{2}} |\nabla_{\text{s}} \mathbf{u}|$ with $\nabla_{\text{s}} \mathbf{u} := \frac{1}{2}(\nabla \mathbf{u} + \nabla \mathbf{u}^{\text{T}})$, and

$$\Phi(\nabla_{\text{s}} \mathbf{u}) = \begin{cases} 2\mu \dot{\epsilon}_{\text{II}}^2 + \frac{\tau_{\text{yield}}^2}{2\mu}, & 2\mu \dot{\epsilon}_{\text{II}} \leq \tau_{\text{yield}}, \\ 2\tau_{\text{yield}} \dot{\epsilon}_{\text{II}}, & \text{otherwise,} \end{cases}$$

with Huber parameters $\alpha = 2\mu$, $\delta = \sqrt{2}\tau_{\text{yield}}$, $\beta = \frac{\delta^2}{2\alpha} = \frac{\tau_{\text{yield}}^2}{2\mu}$; consider

find minimizer $\mathbf{u}^* : (0, 1)^3 \rightarrow \mathbb{R}^3$ of

$$\min_{\mathbf{u}} J(\mathbf{u}) := \int_{\Omega} \Phi(\nabla_{\text{s}} \mathbf{u}) - \mathbf{f} \cdot \mathbf{u} \quad \text{s.t.} \quad \nabla \cdot \mathbf{u} = 0$$

Standard v.s. perturbed Newton linearization

Standard Newton linearization yields the system for step $(\hat{\mathbf{u}}, \hat{p})$:
 (Note: The viscosity in the Newton step is an anisotropic 4th-order tensor.)

$$-\nabla \cdot \left[2 \left(\chi \mu + (1 - \chi) \frac{\tau_{\text{yield}}}{\sqrt{2} |\nabla_s \mathbf{u}|} \left(\mathbf{I} - \frac{\nabla_s \mathbf{u} \otimes \nabla_s \mathbf{u}}{|\nabla_s \mathbf{u}|^2} \right) \right) \nabla_s \hat{\mathbf{u}} \right] + \nabla \hat{p} = -\mathbf{r}_{\text{mom}}$$

$$-\nabla \cdot \hat{\mathbf{u}} = -r_{\text{mass}}$$

Perturbed and reduced Newton linearization of the momentum equation:

$$-\nabla \cdot \left[2 \left(\chi \mu + (1 - \chi) \frac{\tau_{\text{yield}}}{\sqrt{2} |\nabla_s \mathbf{u}|} \left(\mathbf{I} - \frac{\nabla_s \mathbf{u} \otimes \mathbf{S}}{|\nabla_s \mathbf{u}|} \right) \right) \nabla_s \hat{\mathbf{u}} \right] + \nabla \hat{p} = -\mathbf{r}_{\text{mom}}$$

where we defined, for $\mathbf{u} \in H^1(\Omega)^d$ and $\mathbf{S} \in L^\infty(\Omega)^{d \times d}$, $\|\mathbf{S}\|_{L^\infty} \leq 1$,

$$\text{error: } E(\mathbf{u}, \mathbf{S}) := \frac{\nabla_s \mathbf{u}}{|\nabla_s \mathbf{u}|} - \mathbf{S}, \quad \text{perturbation: } D(\mathbf{u}, \mathbf{S}) := \nabla_s \mathbf{u} - |\nabla_s \mathbf{u}| \mathbf{S}$$

Numerical results for Stokes flow with yielding rheology

Numerical comparison of solver convergence for 3D nonlinear Stokes flow.

The model problem smoothly incorporates low-viscosity plumes in a high-viscosity background medium.

Yielding volume	Mesh level ℓ	Standard Newton			Perturbed Newton		
		It. Newton	#backtr.	It. GMRES	It. Newton	#backtr.	It. GMRES
~45%	4	33	20	1469	10	0	379
~45%	5	36	25	2255	12	0	664
~45%	6	57	49	4255	13	0	876
~65%	4	29	21	1559	18	10	965
~65%	5	37	26	2464	17	9	1245
~65%	6	48	39	3892	20	9	1707
~90%	4	35	25	1505	19	11	872
~90%	5	40	32	2147	21	11	1267
~90%	6	32	21	2312	23	11	1811

Outline

Introduction

Derivation of Locally Perturbed Newton Linearizations

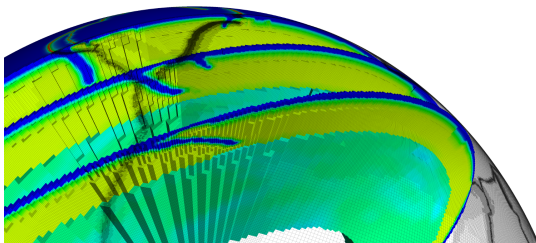
Earth's Mantle Convection: Driving Application & Solver Challenges

Numerical Experiments: Viscoplastic/Multi-Viscosity Stokes Flow

Implications and Outlook for Computational Mantle Flow

Inexact Newton–Krylov with AMR for global mantle models

- ▶ **Robust Newton convergence** w.r.t. nonlinear parameters that is largely independent of the discretization; allows treatment of mantle models in an inverse problem setting.
- ▶ **Grid continuation** at initial Newton steps: Adaptive mesh refinement to resolve increasing viscosity variations arising from the nonlinear rheology.
- ▶ Velocity residual is measured in H^{-1} -norm for **backtracking** line search; this avoids overly conservative update steps $\ll 1$.

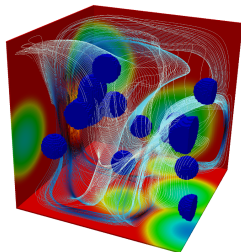
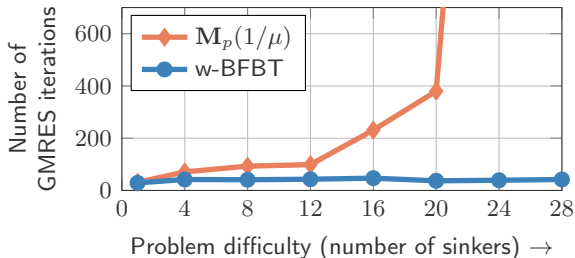


w-BFBT: Robust inverse Schur complement approximation

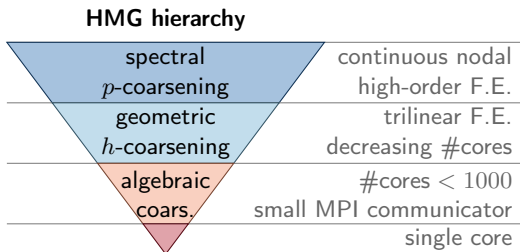
$$\begin{bmatrix} \mathbf{A} & \mathbf{B}^\top \\ \mathbf{B} & \mathbf{0} \end{bmatrix} \begin{bmatrix} \tilde{\mathbf{A}} & \mathbf{B}^\top \\ \mathbf{0} & \tilde{\mathbf{S}} \end{bmatrix}^{-1} \begin{bmatrix} \tilde{\mathbf{u}} \\ \tilde{\mathbf{p}} \end{bmatrix} = \begin{bmatrix} -\mathbf{r}_1 \\ -\mathbf{r}_2 \end{bmatrix} \quad \begin{array}{l} \tilde{\mathbf{A}}^{-1} \approx \mathbf{A}^{-1} \rightarrow \text{MG V-cycle} \\ \tilde{\mathbf{S}}^{-1} \approx (\mathbf{B}\mathbf{A}^{-1}\mathbf{B}^\top)^{-1} \end{array}$$

$$\tilde{\mathbf{S}}_{w\text{-BFBT}}^{-1} := \underbrace{\left(\mathbf{B}\mathbf{C}_w^{-1}\mathbf{B}^\top\right)^{-1}}_{\rightarrow \text{MG V-cycle}} \left(\mathbf{B}\mathbf{C}_w^{-1}\mathbf{A}\mathbf{D}_w^{-1}\mathbf{B}^\top\right) \underbrace{\left(\mathbf{B}\mathbf{D}_w^{-1}\mathbf{B}^\top\right)^{-1}}_{\rightarrow \text{MG V-cycle}}$$

Choice of diagonal weighting matrices $\mathbf{C}_w = \mathbf{D}_w$ is critical for efficacy & robustness [Rudi, Stadler, Ghattas, 2017].

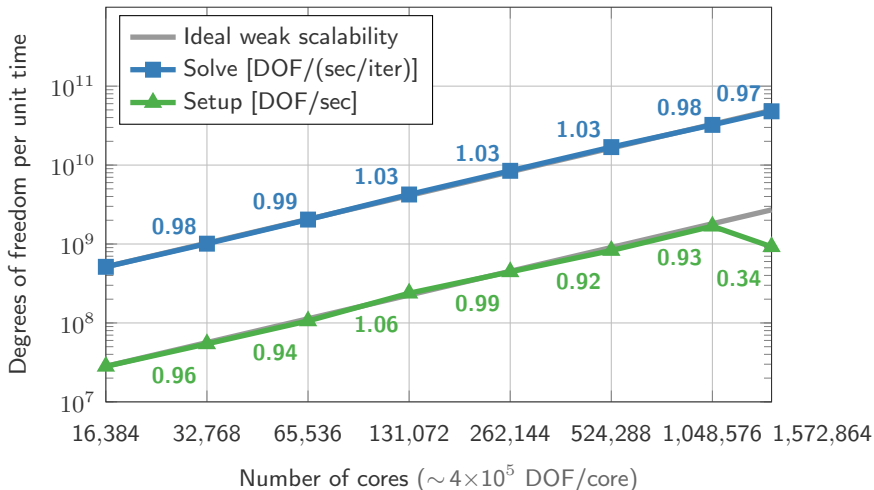


HMG: Hybrid spectral–geometric–algebraic multigrid



- ▶ Multigrid hierarchy of nested meshes is generated from an **adaptively refined octree-based mesh** via spectral–geometric coarsening
- ▶ **Parallel repartitioning** of coarser meshes for load-balancing (crucial for AMR); sufficiently coarse meshes occupy only **subsets of cores**
- ▶ **High-order L^2 -projection** onto coarser/finer levels
- ▶ **Chebyshev accelerated Jacobi smoother** with tensorized matrix-free high-order stiffness apply; assembly of high-order diagonal only

Extreme weak scalability on LLNL's Sequoia supercomputer



Given: Observational data [Collab. with M. Gurnis, Caltech]

- ▶ Current **plate motion** from GPS and magnetic anomalies
- ▶ **Topography** indicating normal traction at Earth's surface
- ▶ **Plate deformation** obtained from dense GPS networks
- ▶ **Average viscosity** in regions affected by post-glacial rebound

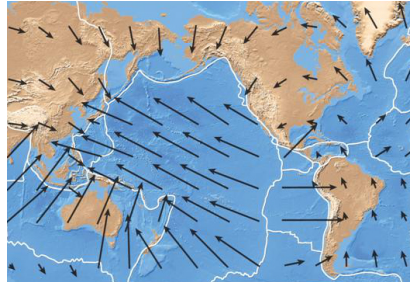


Plate motion (Credit: Pearson Prentice Hall, Inc.)

Additional knowledge contributing to mantle flow models:

- ▶ Location and geometry of plates, **plate boundaries**, and subducting slabs (from seismicity)
- ▶ Images of present-day **Earth structure** (by correlating seismic wave speed with temperature)
- ▶ **Rock rheology** extrapolated from laboratory experiments

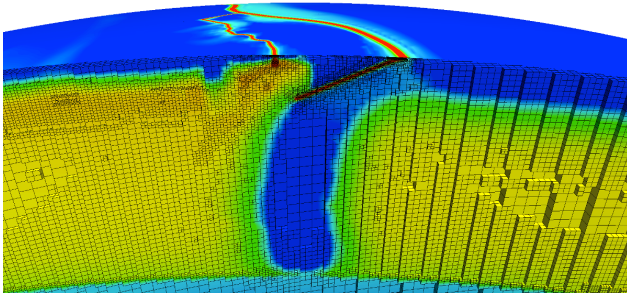
Want: Inversion to constrain parameters of mantle models

Constant rheological parameters affecting viscosity and nonlinearity:

- ▶ **Scaling factor** of the upper mantle viscosity (down to ~ 660 km depth)
- ▶ **Stress exponent** controlling severity of strain rate weakening
- ▶ **Yield strength** governing plastic yielding phenomena

Spatially varying parameters modeling geometry of plate boundaries:

- ▶ **Coupling strength** / energy dissipation between plates



Summary

Focus in today's talk:

- ▶ Our challenge: nonlinear applications modelled by optimization problems with singularities in the Hessian due to a L^1 -norm type term in the objective.
- ▶ Hessian exhibits a null space upon linearization with Newton's method that is problematic for convergence.
- ▶ Applications include inverse problems with total variation regularization as well as viscoplastic/multi-viscosity flows like Earth's mantle convection.
- ▶ We analyze issues with the standard Newton linearization theoretically and through numerical experiments.
- ▶ We propose an improved linearization based on a perturbation of an otherwise implicitly assumed equality constraint.
- ▶ We achieve robust and fast Newton convergence largely independent of the discretization.

Global-scale mantle solver:

- ▶ Hybrid spectral–geometric–algebraic multigrid (builds on p4est library; extended by a coarsening correction to enable coarsening across core boundaries). [Rudi, Malossi, Isaac, et al., 2015]
- ▶ Weighted BFBT preconditioner for the for the Schur complement; scalable HMG-based BFBT algorithms, heterogeneity-robust weighting of BFBT and theoretical foundation. [Rudi, Stadler, Ghattas, 2017]
- ▶ Inexact Newton–Krylov with nonlinear preconditioning and grid continuation for highly nonlinear mantle rheology.
- ▶ Optimal algorithmic performance w.r.t. mesh refinement; nearly optimal w.r.t. higher discretization order.
- ▶ Parallel scalability of solvers to 1.6M cores (collaboration with IBM Research, Zurich). [Rudi, Malossi, Isaac, et al., 2015]